MODELING TIME DISPERSION DUE TO OPTICAL PATH LENGTH DIFFERENCES IN SCINTILLATION DETECTORS*

W.W. Moses, W.-S. Choong, S.E. Derenzo

Lawrence Berkeley National Laboratory Berkeley, CA 94720, USA

(Received August 20, 2014)

We characterize the nature of the time dispersion in scintillation detectors caused by path length differences of the scintillation photons as they travel from their generation point to the photodetector. Using Monte Carlo simulation, we find that the initial portion of the distribution (which is the only portion that affects the timing resolution) can usually be modeled by an exponential decay. The peak amplitude and decay time depend both on the geometry of the crystal, the position within the crystal that the scintillation light originates from, and the surface finish. In a rectangular parallelpiped LSO crystal with 3 mm $\times$ 3 mm cross section and polished surfaces, the decay time ranges from 10 ps (for interactions 1 mm from the photodetector) up to 80 ps (for interactions 50 mm from the photodetector). Over that same range of distances, the peak amplitude ranges from 100% (defined as the peak amplitude for interactions 1 mm from the photodetector) down to 4% for interactions 50 mm from the photodetector. Higher values for the decay time are obtained for rough surfaces, but the exact value depends on the simulation details. Estimates for the decay time and peak amplitude can be made for different cross section sizes via simple scaling arguments.

DOI:10.5506/APhysPolBSupp.7.725
PACS numbers: 29.40.–n, 29.40.Mc, 87.10.Rt, 87.57.uk

1. Introduction

Spurred by the promise of significant performance enhancements in both time-of-flight PET and subatomic particle physics, there have been increasing efforts in recent years to improve the timing resolution of scintillation detectors. As part of this development, there has been a push to quantitatively understand the fundamental limits of timing resolution in scintillation

* Presented at the Workshop on Picosecond Photon Sensors for Physics and Medical Applications, Clermont-Ferrand, France, March 12–14, 2014.

detectors [1–8]. In a recent paper [9], we identified four factors that appear to be the only ones to significantly affect the timing resolution. These are:

1. the initial photoelectron rate (which includes the amount of energy deposited into the scintillator, the scintillation efficiency and decay time, the light collection efficiency of the scintillation detector, and the photodetector quantum efficiency),
2. the intrinsic (exponential) rise time of the scintillator,
3. the transit time jitter of the photodetector,
4. the optical dispersion in the scintillation detector.

Given numerical values for each of these factors, that paper presents a mathematical formula that gives the best timing resolution possible for a scintillation detector with those properties using optimal leading edge threshold discrimination. With the exception of the fourth factor (the optical dispersion), all of these factors are readily obtainable from some combination of the scientific literature and the scintillator and photodetector manufacturers. Thus, the purpose of this paper is to provide quantitative estimates for this final factor.

2. Background and methods

In scintillation detectors, each scintillation photon travels via a unique path to the photodetector. These paths have different lengths, implying that there will be some time dispersion among these photons when they arrive at the photodetector, even if they were all generated at the same location and time. While this optical dispersion is known to affect the timing resolution achievable in scintillation detectors, the magnitude of this dispersion and its dependence on scintillator crystal geometry have not been fully studied. We use Monte Carlo simulation to estimate the nature of this dispersion as a function of the scintillator crystal geometry, the location within the scintillation crystal where the light was produced, and the surface finish.

We perform the simulation using the optical simulation package in Geant4 [10], which was originally the code known as DETECT2000 [11]. We simulate a rectangular parallelpiped geometry with three surface finishes (polished, chemically etched, and rough) covered with a white diffuse reflector. Each of these surface finishes is simulated with two different methods. The first is the "Unified" model, whereby the surface is modeled as being composed of very small facets of specular reflector. These facets are oriented so that the angle between their normals and the macroscopic face are distributed according to a Gaussian distribution, with the standard deviation of this Gaussian given by a user adjustable parameter known as σ_α. For the specular reflector, σ_α is $0°$ (indicating that all of these facets are parallel to the crystal surface), while σ_α is assumed to be $6°$ and $12°$, respectively, for the etched and diffuse finish, based on the results presented by [1, 12]. The polished and covered with Teflon tape, chemically etched, and rough surfaces were also modeled using the "RealSurface" model [13], which is based on measured distributions of the reflection from these surfaces [14–16]. When using the Unified package, the reflector was modeled as Lambertian reflector with 95% reflectivity, and the effects of the reflector are already included in the RealSurface package. The bulk scattering and absorption lengths are assumed to be 20 cm in all cases. While true values for these parameters are not known (there are reports that the attenuation length is > 4000 mm in LSO [17]), the results are essentially identical if 100% reflectivity and infinite absorption and scattering lengths are assumed. This is not surprising, given that the only photons that contribute to the generation of the timing estimator are the first photons to arrive at the photodetector. As these photons travel a comparatively small distance and undergo a comparatively small number of reflections, the values for reflectivity and bulk absorption and scattering properties do not affect the results.

For each simulation, 2.5 million scintillation photons were generated, with the initial position and the direction of travel isotropically distributed within the crystal. Each photon was tracked until it impinged on the photodetector, which was assumed to be 100% absorptive, and the time between the initial emission and the absorption recorded. Figure 1 shows a histogram of the photon arrival times for all those photons that were generated between 14 mm and 16 mm from the photodetector (referred to as "15 mm from the photodetector") in a $3 \times 3 \times 30$ mm^3 LSO crystal with a photodetector coupled to one 3×3 mm^2 end and the remaining five sides polished.

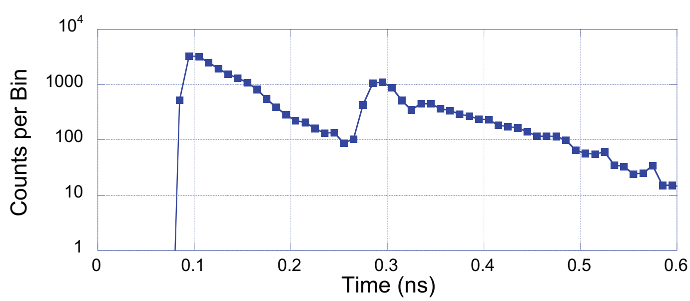

Fig. 1. Distribution of photon arrival times at the photodetector. The photons were generated isotropically between 14 and 16 mm away from the photodetector in a $3 \times 3 \times 30$ mm^3 LSO crystal. The photodetector is on one 3×3 mm^2 end, and the other five sides are simulated as polished and covered with Teflon tape.

One can observe several things from figure 1. First, one notices that the distribution has two peaks. Half of the photons travel toward the photodetector immediately after emission, and the peak near 0.1 ns consists primarily of these photons. Similarly, the peak near 0.3 ns consists primarily of the photons that initially travel away from the photodetector, but reflect off the far end of the crystal and then travel back to the photodetector. As each peak looks reasonably linear when plotted on a semi-logarithmic scale, they can be well represented by an exponential decay with the form

$$I(t) = I_0 \exp(-(t - t_0)/\tau)\,, \tag{1}$$

where $I(t)$ is photon intensity as a function of time, I_0 is the peak amplitude, τ is the "decay time", and t_0 is delay time, as $I(t)$ is zero when $t < t_0$ (with $t = 0$ being the time that the photon was emitted).

3. Results

The data in figure 1 suggest a simplified method for modeling crystals with different lengths, which is shown schematically in figure 2. The full distribution can be thought of as the superposition of two distributions. One distribution is from the photons generated at distance x from the photodetector that initially travel towards the photodetector. In the top portion of figure 2, these are represented as the arrow originating at the dot in the center of the crystal (the emission position) and pointing to the left. The other distribution is due to the photons generated at distance x from the photodetector that initially travel away from the photodetector. In the top portion of figure 2, these are represented as the arrow originating at the emission position and pointing to the right, then reflecting at the end of the crystal and traveling to the photodetector. As the bottom portion of figure 2 shows, this second distribution can be modeled as having been created in an infinitely long crystal, at a position that is $2L - x$ away from the photodetector, and initially traveling toward the photodetector.

As an infinitely long crystal is problematic to model, the data presented below are modeled using a $3 \times 3 \times 50$ mm^3 LSO crystal with a 100% absorptive photodetector on one 3×3 mm^2 end and a 100% absorptive "black" surface at the opposite end. The arrival time distributions obtained this way for interactions occurring at a distance x away from the photodetector (in reality, uniformly distributed in a volume ranging from $x - 1$ mm to $x + 1$ mm from the photodetector) are fit using Eq. (1) and the values for the three fitting parameters (I_0, t_0, and τ) determined. For all cases, t_0 was equal to xn/c, where x is defined as above, n is the index of refraction of LSO scintillator (1.82), and c is the speed of light in vacuum.

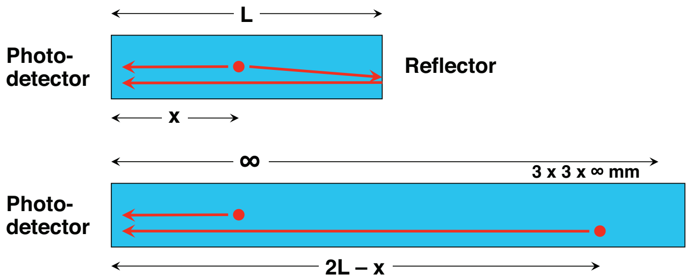

Fig. 2. The simulation of a crystal of length L (with photons emitted both toward and away from the photodetector) can be simplified by simulating emissions from an infinitely long crystal. The photons that reflect at the right side of the crystal in the upper figure follow a path that is equivalent to the photons generated at position $2L - x$ in the lower figure.

Figure 3 shows the fit values for I_0 and τ as a function of distance of the scintillation photons from the photodetector, as well as their product (which is the total number of photons impinging on that photodetector). Two different surface finishes are shown (polished and chemically etched), with each surface finish modeled in two different ways (the Unified model and the RealSurface package). The results for all four of these models give extremely similar results. The decay time increases roughly linearly with distance from the photodetector, ranging from 10 ps when the photons are emitted 1 mm from the photodetector to between 60 ps and 100 ps when the photons are emitted 49 mm from the photodetector. The peak amplitude decreases more rapidly with increasing distance, dropping at 49 mm distance to between 2% and 5% of the peak amplitude at 1 mm distance. The total number of photons impinging on the photodetector decreases roughly linearly with increasing distance, with the drop-off being slightly larger for etched crystals simulated with the RealSurface package than with polished crystals or with etched crystals simulated with the Unified model. This is consistent with what is observed in PET detectors that employ double-ended readout [18–20].

Figure 4 shows similar data for a rough surface. For the simulation of rough surfaces, the Unified model gives results that are similar to the Unified model for polished and etched surfaces, while the RealSurface model has significantly longer decay times (up to 300 ps) and a much faster drop-off in peak amplitude. Also note that data are not presented from the RealSurface model for distances larger than 17 mm. The reason for this is illustrated by figure 4 (c), which shows the shape of the photon arrival time distribution as a function of distance from the emission point to the photodetector is no longer represented well by an exponential decay. For the Unified model, the

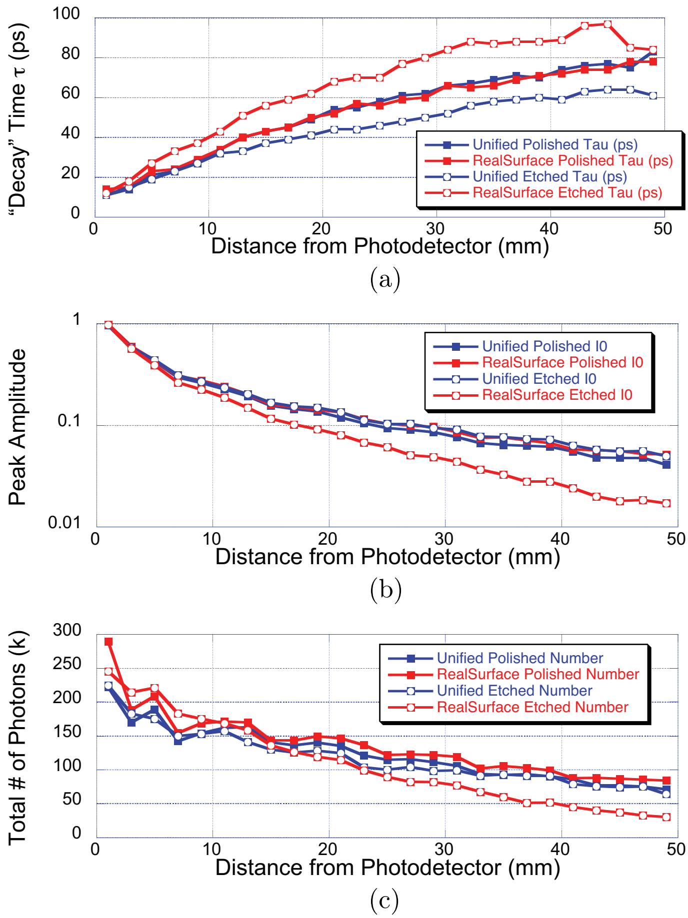

Fig. 3. (a) Fit decay time *versus* distance from the photodetector for two different surface finishes and reflection modeling methods. (b) Fit peak amplitude *versus* distance from the photodetector. (c) Number of photons detected by the photodetector *versus* distance from the photodetector.

shapes are exponential, independent of the emission depth. While the shape is reasonably exponential with the RealSurface package at 5 mm, it can no longer be accurately represented by an exponential for emission distances longer than ~ 15 mm.

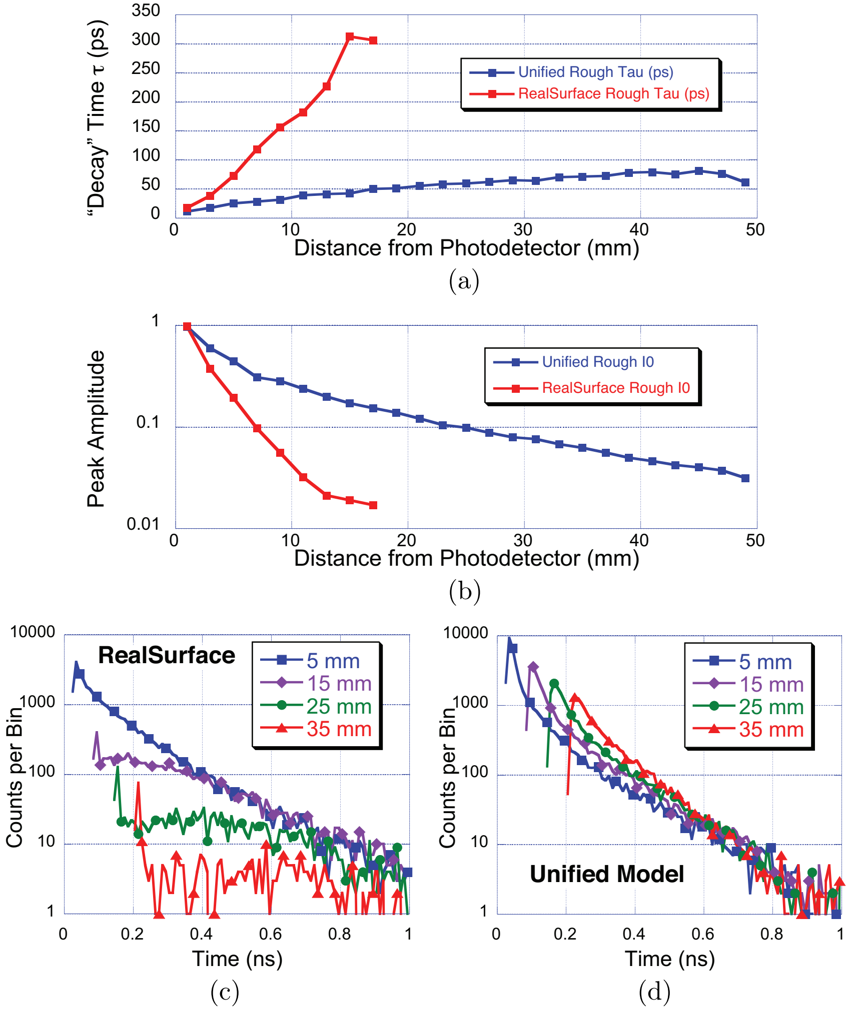

Fig. 4. (a) Fit decay time *versus* distance from the photodetector for a rough surface finishes, modeled with two different reflection modeling methods. (b) Fit peak amplitude *versus* distance from the photodetector. (c) Distribution of the arrival times for photons generated at four different distances from the photodetector, modeled with the RealSurface package. (d) The same as (c), but modeled with the Unified surface reflection model.

4. Discussion

The simulations have shown that for both polished and etched surfaces, the distribution of photons on the face of a photodetector is well described by a single exponential in time. This exponential can be modeled by three parameters: a delay, a decay time, and a peak amplitude, and the values for these three parameters are essentially independent of whether the Unified or RealSurface model is used to simulate the distributions. While the simulations were performed using an LSO scintillator crystal with 3 mm × 3 mm cross section, figure 5 shows that these results can be scaled up to crystals of arbitrary cross section. Consider first a simulation performed on a crystal with cross section w, with a photon emitted at distance x away from the photodetector. The simulation will cause it to follow a path to the photodetector, arriving there a time t after it was emitted. Now consider the simulation of what is essentially the same photon, except that it was emitted in a crystal with cross section kw, where k is an arbitrary scale factor. A photon emitted at distance kx will follow a very similar path to the photodetector, but it will take a time kt to reach the photodetector. In other words, data for a crystal with a square cross section w can be extracted from the curves in figures 3 and 4 merely by multiplying all distances and times in those figures by k, where k is equal to w divided by 3 mm.

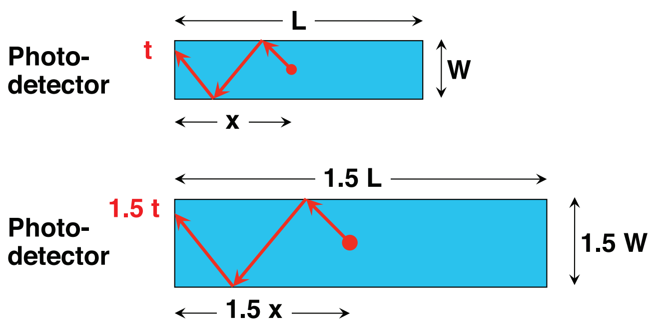

Fig. 5. Scaling method used to convert the results from the $3 \times 3 \times 50$ mm^3 crystal to one with an arbitrarily sized (but square) cross section crystal. In essence, if one increases all the distances involved by a factor of 1.5, the time that it takes for each photon to propagate from the emission point to the photodetector also increases by a factor of 1.5.

The predictions for the Unified and RealSurface models differ significantly only for the rough surface, which can be attributed to the way the simulations are performed. With the Unified model, all reflections are assumed to be quasi-specular; they are specular but from a surface that is not parallel to the macroscopic face. However, the deviations from parallel are relatively small — only 12° for the rough surface and less for the etched and polished surfaces. Thus, it is not surprising that all three surface simulations using the Unified model yield similar results, as they only differ by a few degrees of surface roughness. Although the RealSurface package is based on lookup tables instead of randomly oriented facets, the reflectance distributions used for the polished and etched surfaces are also quasi-specular, and thus very similar to those simulated by the Unified model. Therefore, these five simulations should show similar results. In contrast, the reflectance distributions used by the RealSurface package for the rough surface are extremely broad, nearly the Lambertian distribution. As each photon reflects off the surface at an essentially random angle, its propagation through the crystal is better described as diffusion as opposed to quasi-specular reflection. Thus, the values for the rough surfaces predicted by the Unified and RealSurface models are quite different. Identifying the simulation model that best describes reality requires measurements of timing distributions with ~ 10 ps accuracy or a method for tracking (through measurement, not simulation) individual photon paths through the crystal. These are extremely difficult measurements to perform and well beyond the scope of this paper.

5. Summary and conclusion

In summary, we have used Monte Carlo simulation to predict the transit time dispersion in LSO scintillator crystals caused by path length differences of the optical photons traveling from their point of emission to the photodetector. The distribution is accurately modeled by an exponential decay whose peak amplitude and time depend both on the surface finish and the distance between the emission point and the photodetector. However, this decay time is generally between 10 ps and 100 ps, with the total number of photons impinging on the photodetector (*i.e.*, the product of the decay time and the peak amplitude) falling roughly linearly with distance between the emission point and the photodetector. Although the results were obtained for rectangular parallelpiped crystals with a 3 mm square cross section, simple scaling arguments allow the results to be applied to crystals with square cross sections of arbitrary size. These results should be valuable to those investigating the timing accuracy achievable in scintillation detector systems.

This work is supported in part by the Director, Office of Science, Office of Biological and Environmental Research, Medical Science Division of the U.S. Department of Energy under Contract No. DE-AC02-05CH11231, and in part by the National Institutes of Health, National Institute of Biomedical Imaging and Bioengineering under grants No. R01-EB006085, R01-EB012524, and R21-EB012599.

REFERENCES

[1] W.-S. Choong, *Phys. Med. Biol.* **54**, 6495 (2009).

[2] R. Vinke *et al.*, *Nucl. Instrum. Methods* **A610**, 188 (2009).

[3] S. Seifert *et al.*, *IEEE Trans. Nucl. Sci.* **59**, 190 (2012).

[4] S. Seifert, H.T. van Dam, D.R. Schaart, *Phys. Med. Biol.* **57**, 1797 (2012).

[5] P. Lecoq, *IEEE Trans. Nucl. Sci.* **59**, 2313 (2012).

[6] S. Gundacker *et al.*, *J. Instr.* **8**, 1 (2013).

[7] P. Lecoq, M. Korzhik, A. Vasil'ev, *IEEE Trans. Nucl. Sci.* **61**, 229 (2014).

[8] E. Auffray *et al.*, *IEEE Trans. Nucl. Sci.* **60**, 3163 (2013).

[9] S.E. Derenzo, W.-S. Choong, W.W. Moses, *Phys. Med. Biol.* **59**, 3261 (2014).

[10] S. Agostinelli *et al.*, *Nucl. Instrum. Methods* **A506**, 250 (2003).

[11] F. Cayouette, M. Laurendeau, C. Moisan, *DETECT2000: An Improved Monte-Carlo Simulator for the Computer Aided Design of Photon Sensing Devices*, Proc. SPIE, vol. 4833, p. 69, 2003.

[12] A. Levin, C. Moisan, *A More Physical Approach to Model the Surface Treatment of Scintillation Counters and its Implementation into DETECT*, Proc. of The IEEE 1996 Nuclear Science Symposium, pp. 702–706, Edited by A. Del Guerra, Anaheim, CA, 1996.

[13] M. Janecek, W.W. Moses, *IEEE Trans. Nucl. Sci.* **NS-57**, 964 (2010).

[14] M. Janecek, W.W. Moses, *IEEE Trans. Nucl. Sci.* **NS-55**, 1381 (2008).

[15] M. Janecek, W.W. Moses, *IEEE Trans. Nucl. Sci.* **NS-55**, 2432 (2008).

[16] M. Janecek, W.W. Moses, *IEEE Trans. Nucl. Sci.* **NS-55**, 2443 (2008).

[17] C. Moisan, D. Vozza, M. Loope, *IEEE Trans. Nucl. Sci.* **44**, 2450 (1997).

[18] J.S. Huber *et al.*, *Nucl. Instrum. Methods* **437**, 374 (1999).

[19] W.W. Moses, S.E. Derenzo, C.L. Melcher, R.A. Manente, *IEEE Trans. Nucl. Sci.* **NS-42**, 1085 (1995).

[20] Y.F. Yang *et al.*, *Phys. Med. Biol.* **51**, 2131 (2006).